Journal of Ceramic Processing Research. Vol. 13, No. 2, pp. 164~169 (2012)

J O U R N A L O F
Ceramic Processing Research

A systematic investigation of experimental conditions on the particle size and structure of TiO_2 nanoparticles synthesized by a sol-gel method

Roohollah Azizi[a,c]*, Sousan Rasouli[b], Naghi Parvini Ahmadi[c], Amin Jafari jafar kolaei[d] and Mohammad Azizi[e]
[a]*Nanometrology Center, Tehran, Iran*
[b]*Department of Nanomaterials & Nanocoatings, Institute for Color Science and Technology (ICST), Tehran, Iran*
[c]*Engineering Faculty of Nanomaterials, Sahand University of Technology, Tabriz, Iran*
[d]*Puladamin Company, Tehran, Iran*
[e]*Islamic Azad University, Science and Research Branch, Tehran, Iran*

TiO_2 nanoparticles were prepared by a sol-gel method using $TiCl_4$ as a precursor. The effect of the $TiCl_4/H_2O$ molar ratio and DBS/ethanol (two important parameters in this process) on the particle size and structure of the samples were studied. The structure and morphology of the nanoparticles were investigated by X-ray diffraction, scanning electron microscopy and transmission electron microscopy. A systematic study was made by using the results of Design-Expert software. The optimum ratio of $TiCl_4/H_2O$ and DBS/ethanol, to achieve the smallest particle size and the highest rutile content, were studied. Results showed that a lower $TiCl_4/H_2O$ molar ratio led to smaller nano particles and that this goal is achieved for the lowest $TiCl_4/H_2O$ molar ratio and intermediate DBS/ethanol values.

Key words: TiO_2 nano pigment, sol-gel method, $TiCl_4$ precursor.

Introduction

TiO_2 nanoparticles are interesting by scaling because of their unique photocatalyst properties.

In order to prepare TiO_2 nanoparticles with satisfactory properties several processes have been developed over the last decade and can be classified as a liquid process (sol-gel [1-4], solvothermal [5, 6], hydrothermal [7, 8]), solid state processing routes (mechanical alloying/milling [9, 10], mechanochemical [11, 12]), RF thermal plasma [13] and other routes such as laser ablation [14].

The sol-gel method is widely used for the preparation of TiO_2 nano powder. The sol-gel method is a wet-chemical technique for the fabrication of nano materials starting either from a chemical solution or colloidal particles to produce an integrated network. Typical precursors are metal alkoxides and metal chlorides, which undergo hydrolysis and polycondensation reactions to form a colloid, a system composed of solid particles (size ranging from 1 nm to 1 µm) dispersed in a solvent. The sol evolves then towards the formation of an inorganic continuous network containing a liquid phase (gel).

Many studies have been made about the effect of various factors such as the peptization process, the amount of hydrolysis retardant acetylacetone, the pH value of the sol, the sol aging time, the calcination temperature and a surfactant on the sol-gel process [15-23]. $TiCl_4/H_2O$ and DBS/ethanol are two important parameters in this process.

Design-Expert software was used to define an optimal combination for the factors affecting an experiment [19]. The aim of this method is to determine the system sensitivity to each parameter. This method is quite beneficial because the behavior of a system can be easily verified depending on the factors incorporated [20].

In this study, TiO_2 nano particles were prepared via a sol-gel method using $TiCl_4$ as a precursor. The effect of the $TiCl_4/H_2O$ molar ratio and DBS/ethanol on the particle size and structure of the powders were investigated. The products are characterized by X-ray diffraction (XRD), scanning electron microscopy (SEM) and transmission electron microscopy (TEM).

Experimental

Materials and methods

Titanium chloride ($TiCl_4$, 99%) and ethanol were sourced from Merck and dodecyl benzene sulfonate (DBS) was sourced from Acros. TiO_2 nanoparticles were obtained through the hydrolysis of titanium precursors, $TiCl_4$. Table 1 presents the experimental conditions for 9 runs. Experiments were performed according to the conditions in Table 1. In all of the experiment, deionized water was used with $TiCl_4$ in the $TiCl_4/H_2O$ molar ratio from Table 1. The surfactant (DBS) was dissolved in ethanol; then the DBS/ethanol was added into the titanium precursor solution, slowly (titanium/DBS/ethanol molar ratio = 1 : 1 : 10, 0.5 ml/minute). Then the mixture of precursor and surfactant was added

*Corresponding author:
Tel : +989126595922
Fax: +982176250050
E-mail: azizi.roohollah@gmail.com

Table 1. 9 different experimental condition were designed by the Design-Expert software

Run	A:$TiCl_4/H_2O$ (Molar ratio)	B:DBS/ethanol (Wt %)
1	0.04	8.61
2	0.05	5.25
3	0.04	1.89
4	0.03	5.25
5	0.03	10
6	0.02	1.89
7	0.02	8.61
8	0.01	5.25
9	0.03	0.5

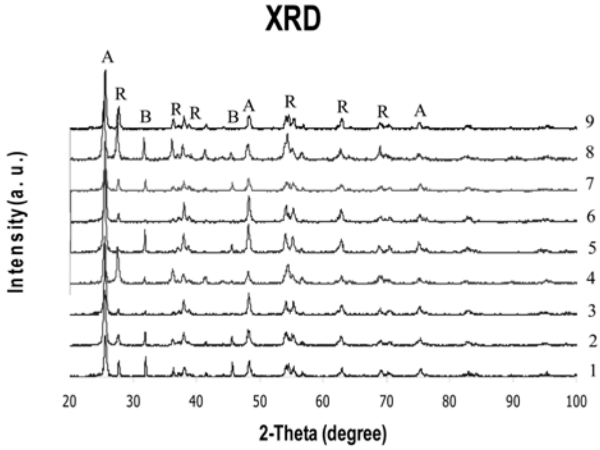

Fig. 1. XRD patterns of the powders after calcination at 700 °C.

into the mixture of deionized water and ethanol slowly (titanium/H_2O/Ethanol molar ratio = 1 : 4 : 10, 0.5 ml/minute). An hydrolysis reaction and polymerization took place in this mixture and a TiO_2 sol was formed. After gelation for 24 h, the gel was dried at 70 °C in an oven until a yellow mass was observed. Calcination of the yellow mass was performed in a chamber furnace at 700 °C for 2 hours.

A D-500 (Siemens, Karlsruhe, Germany) diffractometer was used for the XRD analysis. Morphological analysis was performed using a LEO 1455VP (Oxford, UK) scanning electron microscope (SEM) and an EM 900 (Zeiss) transmission electron microscopy (TEM).

Experimental design

In order to investigate and optimize $TiCl_4/H_2O$ and DBS/ethanol (two important parameters in this process), Experimental Design software was used. To achieve the smallest particle size and the highest rutile content, it is necessary to optimize $TiCl_4/H_2O$ and DBS/ethanol. Therefore, the response surface mode of Design-Expert software was used. Table 1 represents 9 different experimental conditions designed by the Design-Expert software.

Results and Discussion

Structure and morphology

Based on the experimental conditions of Table 1, 9 different experiments were designed. The powders obtained were calcined at 700 °C for 2 h and were characterized by X-ray diffraction.

Fig. 1 presents the X-ray diffraction patterns of the as-synthesized samples. As Fig. 1 shows polycrystalline TiO_2 powders were obtained during calcination step for all samples. Both anatase and rutile phases, according to JCPDS 01-071-1167 and 01-076-0319 cards respectively are observed in the XRD patterns.

Rutile phase calculation

The percentage of rutile and anatase phases can be calculated by equation 1 [21, 22]:

$$x = \frac{1}{\left[1+0.8\left(\frac{I_A}{I_R}\right)\right]} \tag{1}$$

where x is the weight percentage of the rutile phase, I_A and I_R are the peak intensity of the (101) and (110) planes for the anatase and rutile phase, respectively. Table 2 shows the percentage of the rutile phase for each sample after 2 h of calcination at 700 °C. Results reveal that sample 4 has the highest percentage of the rutile phase. However, a pure rutile phase is not obtained completely for the 9 experiments which way caused by non sufficient calcination time or temperature.

Measurement of average particle size by IMAGE PROCESSING analysis:

Fig. 2 shows SEM images of TiO_2 powders synthesized based on the different conditions in Table 1. These images

Table 2. quantity of the rutile phase after 2 h calcination at 700 °C and average particle size by IMAGE PROCESSING analysis

Run	A:$TiCl_4/H_2O$ (Molar ratio)	B:DBS/ethanol (Wt %)	Particle size (nm)	X: mass fraction of rutile (%)
1	0.04	8.61	98	39
2	0.05	5.25	68	21
3	0.04	1.89	54	8
4	0.03	5.25	42	53
5	0.03	10	50	7
6	0.02	1.89	40	13
7	0.02	8.61	32	28
8	0.01	5.25	32	52
9	0.03	0.5	44	37

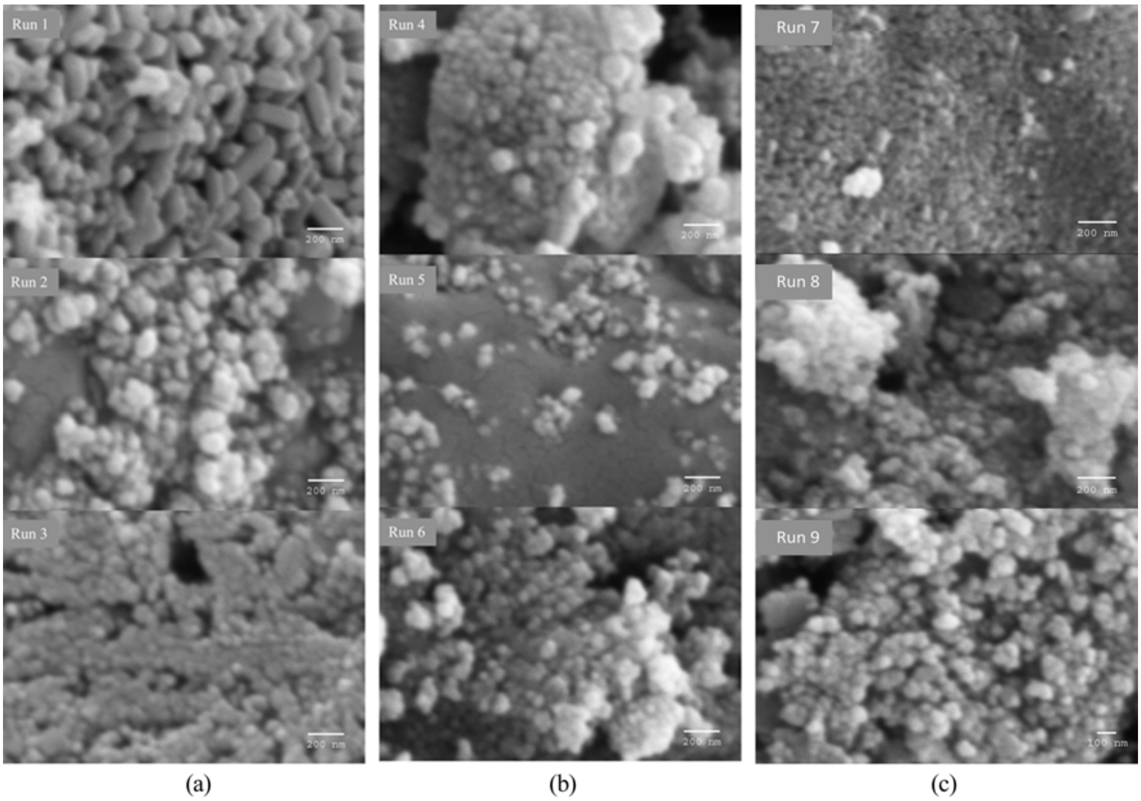

Fig. 2. SEM images taken from samples synthesized based on the different conditions in Table 1.

reveal that the shape of the particles is influenced by the experimental conditions and varied from spherical to elongated. SEM micrographs of the microstructures of all samples were analyzed by IMAGE PROCESSING analysis to obtain the average particle size of the samples.

Experimental design analysis

Table 2 gives the particle size and mass fraction of the rutile phase (two responses of the system) for the 9 runs. The optimum ratio of $TiCl_4/H_2O$ and DBS/ethanol, to achieve the smallest particle size and the highest rutile content**,** were determined by Design-Expert software.

Fig. 3 shows the particle size curve vs. $TiCl_4/H_2O$ molar ratio (water content). This figure shows that decreasing the $TiCl_4/H_2O$, causes a decrease in the particle size. Previous studies demonstrated that the size, stability, and morphology of the sol produced from alkoxide, is strongly affected by the water to titanium molar ratio ($r = [H_2O]/[Ti]$) [16, 17]. Formation of colloidal TiO_2 at a high r ratio is of great interest, because small size particles are formed in this condition [16].

Fig. 4 illustrates the particle size variations vs. DBS/ethanol. As can be seen, this parameter does not greatly affect the particle size evolution.

Fig. 5 shows the interaction of two factors, $TiCl_4/H_2O$ and DBS/ethanol, on the particle size. Each curve can be used to calculate the required levels of $TiCl_4/H_2O$ and

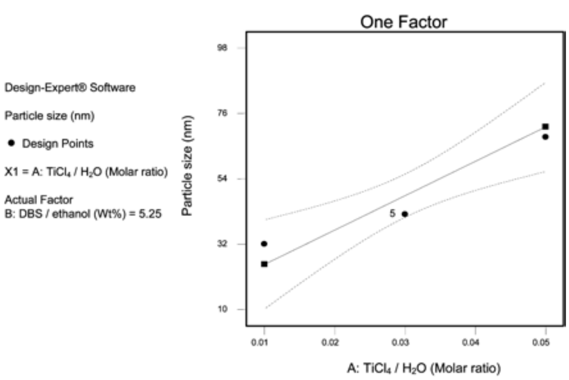

Fig. 3. Shows the particle size curve vs. $TiCl_4/H_2O$.

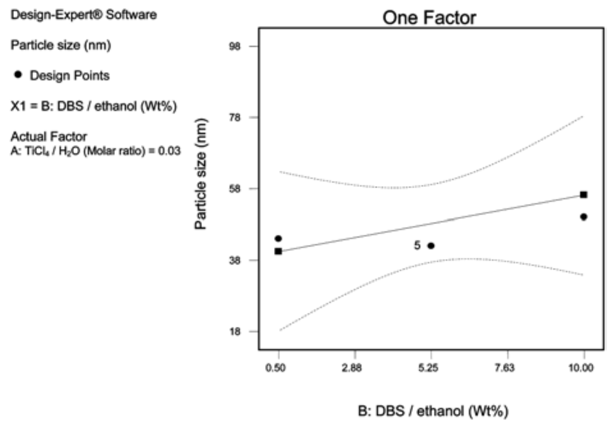

Fig. 4. Illustrates the particle size changes vs. DBS/ethanol.

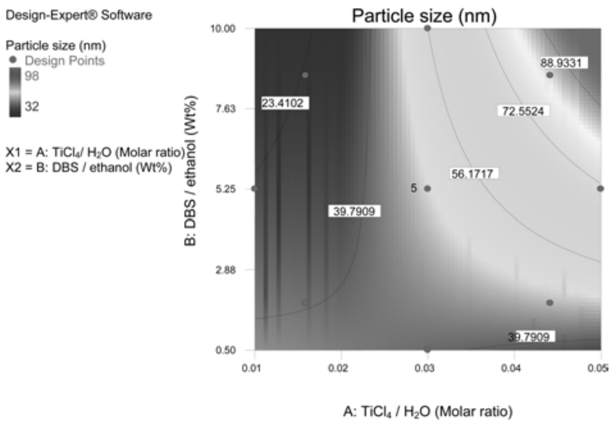

Fig. 5. Shows the effects of $TiCl_4/H_2O$ and DBS/ethanol on the particle size.

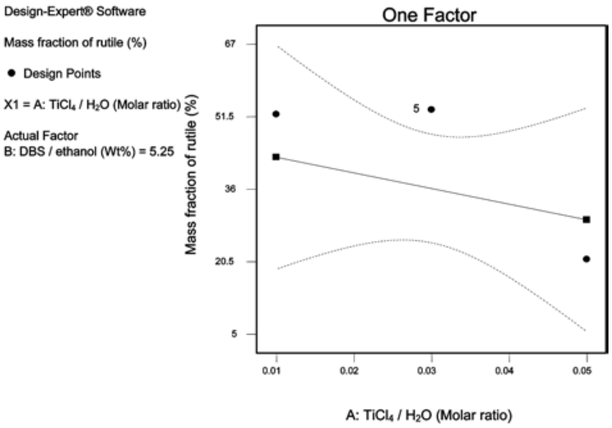

Fig. 6. Illustrates the mass fraction of rutile (%) changes vs. $TiCl_4/H_2O$.

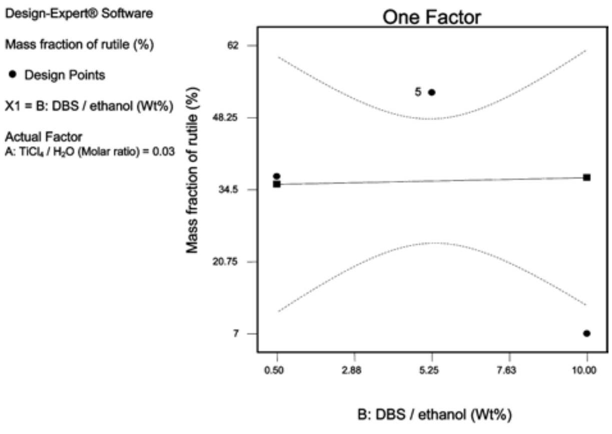

Fig. 7. Illustrates the mass fraction of rutile (%) changes vs. DBS/ethanol.

DBS/ethanol to achieve a certain particle size. From Fig. 5 it can be observed that for the smallest particle size, the lowest level of $TiCl_4/H_2O$ and the highest level of DBS/ethanol are required.

Fig. 6 shows the mass fraction of rutile curve vs. $TiCl_4/H_2O$ (water content). This figure shows that decreasing

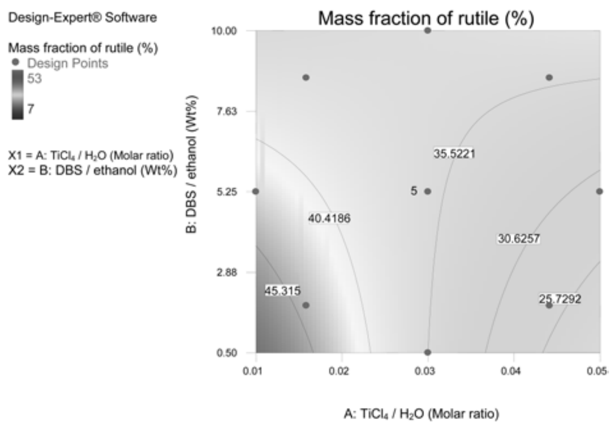

Fig. 8. Shows the effect of the two parameters on the rutile content.

$TiCl_4/H_2O$ causes an increase in the mass fraction of rutile. The main reason is the relationship between the particle size and the anatase-to-rutile transformation. In fact, the anatase-to-rutile phase transformation temperature shifted to a very low level when the crystallite size decreases due to the high surface energy of the particles [16]. Then it is possible to assume that the growth of the rutile-phase-particle starts right after its nucleation.

The effect of the surfactant addition on the phase formation of the TiO_2 nanoparticles was investigated and Fig. 7 shows the results. Fig. 7 reveals that the surfactant content does not have any significant effect on the rutile phase which is also in good agreement with previous results [17].

Fig. 8 shows the effect of the two parameters $TiCl_4/H_2O$ and DBS/ethanol on the mass fraction of rutile. The highest amount of the rutile phase is observed at the lowest values of $TiCl_4/H_2O$ which confirms the results of Fig. 7 and the fact that the surfactant does not affect rutile contents. It can be seen that the rutile phase content is higher at lower values of $TiCl_4/H_2O$.

Fig. 9 represents the optimum ratios of $TiCl_4/H_2O$ and DBS/ethanol, to achieve the smallest particle size and the highest rutile content. The results demonstrate that these goals can be achieved with the lowest $TiCl_4/H_2O$ and intermediate DBS/ethanol values. Fig. 10 shows the optimum ratios of $TiCl_4/H_2O$ and DBS/ethanol, to achieve the smallest particle size and the highest rutile phase must be 0.01 and 3.46, respectively.

Based on the optimum values for the influencing factors the experiments were performed. Fig. 11 and Fig. 12 show good agreement in particle size and rutile phase contents which were 31.99 nm and 45.6%.

Conclusions

TiO_2 nano particles were prepared by a sol-gel method with $TiCl_4$ as a precursor. A mixture of anatas and rutile phases were obtained after calcination at 700 °C for all

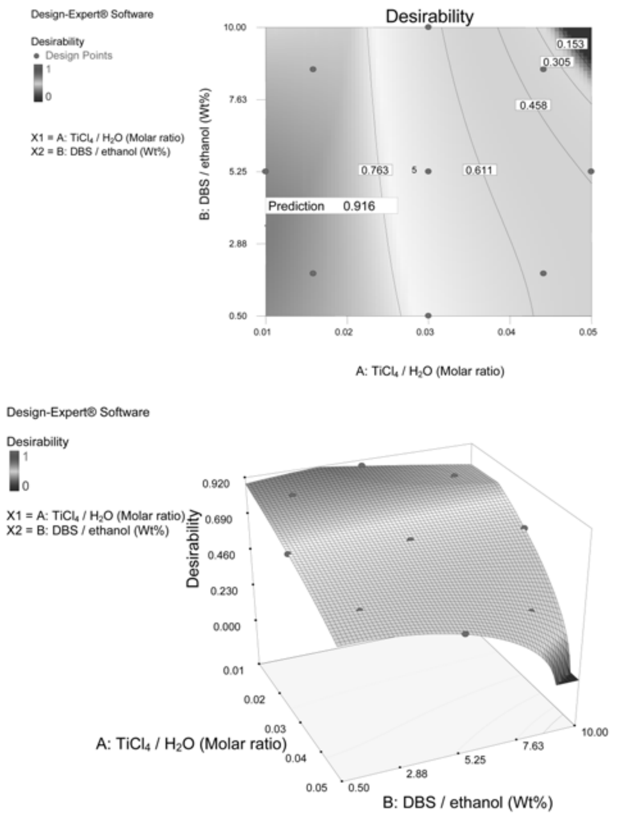

Fig. 9. Optimum $TiCl_4/H_2O$ and DBS/ethanol proportions to achieve the smallest particle size and the highest rutile content.

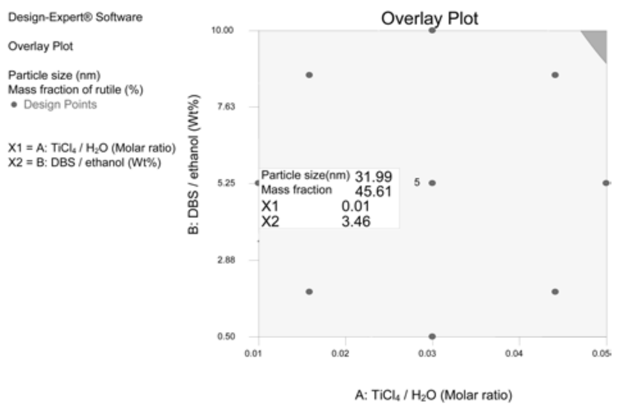

Fig. 10. Optimum $TiCl_4/H_2O$ and DBS/ethanol values.

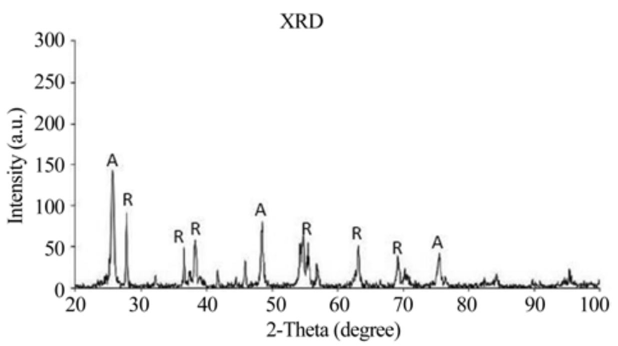

Fig. 11. XRD patterns of desirable powders after calcination at 700 °C.

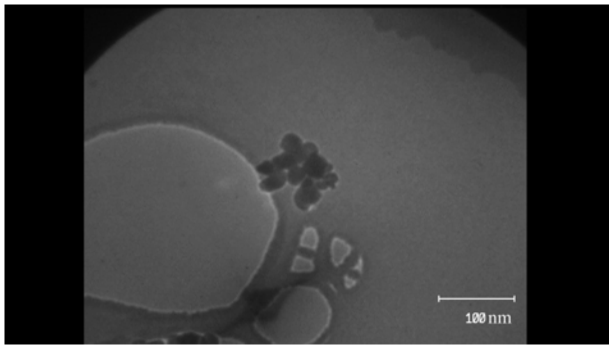

Fig. 12. TEM images of the desirable powder after calcination at 700 °C.

the samples.

The quantitative analysis showed a maximum of the rutile phase, after calcination at 700 °C, for samples 4 and 8. SEM images revealed that the shape of the particles is influenced by the experimental conditions and varied from spherical to elongated. The average particle size calculated with image processing software was between 32 and 98 nm. The optimum ratios of $TiCl_4/H_2O$ and DBS/ethanol (two important parameters in this process), to achieve the smallest particle size and the highest rutile content, were studied. Results showed that a lower $TiCl_4/H_2O$ molar ratio led to the smaller nano particles and that this goal is achieved for the lowest $TiCl_4/H_2O$ and intermediate DBS/ethanol values.

References

1. T. Trung, W.-J. Cho and C.-S. Ha, Mater. Lett. 57 (2003) 2746-2750.
2. T. Sugimoto, X. Zhou and A. Muramatsu, J. Colloid Interface Sci. 252 (2002) 339-346.
3. T. Sugimoto, X. Zhou and A. Muramatsu, J. Colloid Interface Sci. 252 (2002) 347-353.
4. P. Arnal, R.J.P. Corriu, D. Leclercq, P.H. Mutin and A. Vioux, Chem. Mater. 9 (1997) 694-698.
5. C.-S. Kim, B.K. Moon, J.-H. Park, S.T. Chung and S.-M. Son, J. Cryst. Growth 254 (2003) 405-410.
6. C.-S. Kim, B.K. Moon, J.-H. Park, B.-C. Choi and H.-J. Seo, J. Cryst. Growth 257 (2003) 309–315.
7. J.-N. Nian and H. Teng, Hydrothermal synthesis of single-crystalline anatase TiO2 nanorods with nanotubes as the precursor, J. Phys. Chem. B 110 (2006) 4193-4198.
8. Y.V. Kolen'ko, B.R. Churagulov, M. Kunst, L. Mazerolles and C. Colbeau- Justin, Appl. Catal. B: Environ. 54 (2004) 51-58.
9. D.H. Kim, H.S. Hong, S.J. Kim, J.S. Song and K.S. Lee, J. Alloys Compd. 375 (2004) 259-264.
10. P. Xiaoyan and M. Xueming, Mater. Lett. 58 (2004) 513-515.
11. J.L. Guimaraes, M. Abbate, S.B. Betim and M.C.M. Alves, J. Alloys Compd. 352 (2003) 16-20.
12. M. Kamei and T. Mitsuhashi, Surf. Sci. 463 (2000) L609-L612.
13. S.-M. Oh and T. Ishigaki, Thin Solid Films 457 (2004) 186-191.
14. M. Matsubara, T. Yamaki, H. Itoh, H. Abe and K. Asai, J.

Appl. Phys. 42 (5A Pt 2) (2003) L479-L481.
15. T. Troczynski and Q. Yang, U.S. Pat. No. 6,284,682, May, 2001.
16. S. Mahshid a, M. Askari a and M. Sasani Ghamsari, Journal of Materials Processing Technology, 2007, 189, 296-300.
17. D.L. Liao and B.Q. Liao, Journal of Photochemistry and Photobiology A: Chemistry, 2007, 187, 363-369.
18. US Patent, patent number 007326399 B2 Feb.5,2008.
19. Lei Sun, Taicheng An, ShungangWan, Guiying Li, Ningzhong Bao, Xiaohong Hu and Jiamo Fu, Guoying Sheng, Separation and Purification Technology 68 (2009) 83-89.
20. Roesler, R. Richard, Paint Coat. Ind. 50 (July) (2004) 98-104.
21. Qinghong Zhang, Lian Gao and Jingkun Guo, Journal of the European Ceramic Society, 20 (2000) 2153-2158.
22. Yuanzhi Li, Yining Fan and Yi Chen, J. Mater. Chem., 12 (2002) 1387-1390.
23. Xiaobo Chen and Samuel S. Mao, Chem. Rev. 107 (2007) 2891-2959.